



IMPROVED ELECTRON NEUTRINO BEAM

S. Mori

February 24, 1978

I. Introduction

An electron neutrino beam¹ was designed by modifying the existing Sign Selected Bare Target (SSBT) train by S. Mori, S. Pruss and R. Stefanski². In this report I will optimize the previous design under the following assumptions:

- (1) the existing target tube, decay pipe and locations of the neutrino detectors can not be changed,
- (2) the electron neutrino beam train is installed in the target tube,
- (3) conventional and readily available magnets are used,
- (4) the train can run for the total number of protons on the target of the order of 10^{19} or more at 400 and 500 GeV,
- (5) the train can be used for the Energy Doubler operation at 1000 GeV with minor modifications only, and
- (6) the construction cost is modest.

The source of electron neutrinos is the K_L^0 decay

$$K_L^0 \rightarrow \pi^- e^+ \nu_e \text{ and } \pi^+ e^- \bar{\nu}_e \text{ (BR=39\%).} \quad (1)$$

Therefore, ν_e and $\bar{\nu}_e$ fluxes are identical. Muon neutrinos are background in this beam. The major processes³ for muon neutrino backgrounds are

$$K_L^0 \rightarrow \pi^- \mu^+ \nu_\mu \text{ and } \pi^+ \mu^- \bar{\nu}_\mu \text{ (BR=27.5\%)} \quad (2)$$

$$\pi^\pm \rightarrow \mu^\pm \nu_\mu, \mu^\mp \bar{\nu}_\mu \quad (100\%) \quad (3)$$

$$K_S^0 \rightarrow \mu^\pm \nu_\mu, \mu^\mp \bar{\nu}_\mu \quad (63.5\%) \quad (4)$$

$$K_S^0 \rightarrow \pi^+ \pi^- \rightarrow \mu^+ \nu_\mu \mu^- \bar{\nu}_\mu \quad (68.3\%) \quad (5)$$

$$\Lambda \rightarrow p \pi^- \rightarrow p \mu^- \bar{\nu}_\mu \quad (64.2\%) \quad (6)$$

The background from the K_L^0 decay is intrinsic and can not be avoided in the present design. Thus, the design goal is to maximize electron neutrino fluxes and minimize muon neutrino backgrounds from processes (3) through (6) so that they become insignificant compared to the muon neutrinos from the K_L^0 decay.

Optimization was made for the 15-Foot Bubble Chamber with the fiducial radius of 1.35 m at 400 GeV. In the last section computed electron neutrino fluxes and backgrounds for the final design will be shown at 500 and 1000 GeV. The $\bar{\nu}_\mu$ background from the Λ decay becomes dominant at 1000 GeV and cannot be suppressed by any magnet arrangement in the present target tube. A possible solution to this problem will be discussed incorporating the expansion program of the present target tube in the Energy Doubler project. Also shown will be electron neutrino fluxes at the Wonder Building.

II. Electron Neutrino Flux

The ν_e (or $\bar{\nu}_e$) flux is solely determined by apertures of various beam components which will be used to suppress backgrounds and absorb K_L^0 's before they decay. Figure 1 shows ν_e fluxes computed by a Monte Carlo program for various horizontal and vertical apertures. The incident proton energy is 400 GeV. The K_L^0 production cross section is assumed to be the average K^+ and K^- cross sections. Stefanski-White's parametrization⁴ for pion and kaon production was used throughout the presnet study. The fluxes are computed at the 15-Ft. Bubble Chamber and averaged over the radius of 1.35 m. For apertures greater than ± 4 mrad the ν_e flux does not increase. The flux is reduced by about 10% for apertures of ± 2.5 mrad. Therefore, it would be desirable to have apertures of at least ± 2.5 mrad.

Also shown is the ν_e flux under the assumption that the decay pipe has a larger radius and does not absorb K_L^0 's. It should be pointed out that the shape of the spectrum corresponds

roughly to the ν_e , $\bar{\nu}_e$, ν_μ , and $\bar{\nu}_\mu$ spectra from the K_L^0 decay in the dump experiment and it has much softer energy distribution.

III. Muon Neutrino Backgrounds from the π^\pm and K^\pm Decays

Backgrounds from decays of long-lived charged particles ($\tau > 10^{-10}$ sec) can be reduced by a sweeping magnet which follows the target directly. The distance between the target and the upstream end of the magnet (the magnet distance), D , must be kept as short as practical. We consider only the background from the π^+ and K^+ decays in this section, since the background from the π^- and K^- decays are much smaller because of smaller π^- K^- production cross sections. Any other known charged particles can safely be neglected. Figure 2 shows computed ν_μ backgrounds as a function of the neutrino energy for two magnet lengths of 3 m and 6 m magnets. The apertures of ± 2 mrad were used in the horizontal and vertical planes. The magnetic fields were varied from 10 kG to 30 kG. The background suppression is better for the higher fields, since charged particles are bent away sooner after leaving the target. As far as the magnet length is concerned, the length of 6 m was shown to be sufficient when the field is greater than 15 kG.

If only existing magnets are to be used, either of the 6 m long Main Ring bending magnets, 5-1.5-240 or 4-2-240 at 18 kG, is a good compromise. The magnet distance, D , was 0.8 m for the SSBT train. The upstream EPB dipole survived in the last run of 3.7×10^{18} protons on the target at 400 GeV. Since the coil arrangement of the Main Ring dipole magnets is superior to that of the EPB magnets, the magnet distance can be made shorter. The 350 GeV/c Dichromatic Train has the magnet distance of about 0.3 m. Running experience from this beam will help in determining this parameter.

A better scheme is to use a short and narrow aperture magnet of high field directly after the target. Such a magnet can be

designed to make the magnet distance very short and be built at modest cost.

IV. Muon Neutrino Backgrounds from the K_S^0 Decay

The ν_μ and $\bar{\nu}_\mu$ backgrounds from the K_S^0 decay are identical. The K_S^0 cross section is assumed to be the average K^+ and K^- cross sections. Energy distributions for pions, K_S^0 's and pions from the K_S^0 decay are shown in Figure 3 for the polar angle of particle production less than 5 mrad. The incident proton energy is 400 GeV. The pion fluxes from the K_S^0 decay are about 15 and 30 times less than directly produced negative and positive pions, respectively, above 100 GeV. Also shown are energy distributions of Λ production and negative pions from the Λ decay. The details of the Λ production and decay will be discussed in the next section.

The K_S^0 and Λ decay distributions as a function of the distance from the target are shown in Figure 4. All the K_S^0 's and Λ 's which are produced within the polar angle of 5 mrad at 400 GeV are integrated. The Λ decay distribution will be discussed later. The K_S^0 decay distribution indicates that sweeping magnets are needed quite far away from the target. The ν_μ background computed by a Monte Carlo program is shown in Figure 5 for various magnet arrangements. For ease of computation magnets were assumed to have no aperture limitation and apertures were limited only by collimators C1, C2, and C3 to ± 2 mrad in this background study. A single Main Ring dipole magnet was used at the target. A group of magnets which are placed about 20 m from the target can be of the 6-3-120 type which gives an aperture of ± 2 mrad by ± 4 mrad. The third group of magnets must have a large aperture and can be 8-8-60 magnets which were built for the Narrow Band Horn Train. The maximum field of this magnet is 4 kG. N_1 , N_2 , and N_3 indicated in Figure 5 are numbers of magnets used for background calculations of the three places.

The backgrounds for $N_2 = 1$ and 2 are essentially the same when the other conditions are identical. The backgrounds for $N_2 = 0$ (absent) are substantially worse. Therefore, a single 6-3-120 magnet arrangement is reasonable at the middle. The acceptable arrangement seems to be $N_1 = 1$, $N_2 = 1$, and $N_3 = 2$.

V. Muon Antineutrino Background from the Λ Decay

The Λ decay yields only $\bar{\nu}_\mu$ background. Inclusive production of Λ has been measured for 300 GeV protons on beryllium⁵. Functions of the form

$$\sigma(x, t) \big|_{\text{fixed } \theta} = E \frac{d^3\sigma}{dp^3} = \beta(t) (1-x)^{1-2\alpha(t)}$$

were found to give good fits to the data, where $x = 2p_{11}/\sqrt{s}$, p_{11} = the longitudinal component of the Λ momentum in the c.m. system, and t and s are the conventional kinematical variables. The inclusive Λ production at higher energies was assumed to have the same invariant cross section.

The energy distributions of Λ 's and negative pions from the Λ decay, and the decay distance of Λ 's from the target at 400 GeV were shown in Figures 3 and 4. The polarization of Λ has been neglected. The Λ gives a much softer energy distribution of negative pions, but the average decay distance is considerably longer than the K_S^0 . Most importantly, the production cross section of high energy Λ 's in the forward direction is very large.

Figure 6 shows $\bar{\nu}_\mu$ background fluxes for various magnet arrangements. The energy scale was doubled to see more detail. As expected from the decay distance curve the acceptable arrangement for the K_S^0 background does not give a satisfactory result. Two more 8-8-60 magnets reduce the background slightly ($N_1N_2N_3 = 114$). In order to evaluate background contribution from Λ 's which decay in the decay pipe, the last set of magnets were moved downstream to the end of the target tube and the C3 collimator which follows the last magnet was closed. The difference between two broken curves for $N_1N_2N_3 = 112$ is this contribution

which is far more than half of the total background with the C3 open. The bottom curve corresponds to the background when the target is placed inside the first magnet and the C1 collimator is closed.

The optimum solution seems to place the 8-8-60 magnets at the end of the target tube. More than two 8-8-60 magnets certainly helps suppressing the background but the gain is insignificant. Although the aperture of the 8-8-60 magnet is 8" by 8" for a good field volume, the physical horizontal aperture is 18".

VI. Final Design

The schematic diagram of the final electron neutrino beam design is shown in Figure 7. Compared to the previous design of the modified SSBT Train the present design gives smaller muon neutrino backgrounds from the K_S^0 and Λ decays. The M1-1 magnet is very effective in suppressing backgrounds from pions and kaons produced at the target. The M1-2 magnet can be 3 m long as far as the background is concerned, but the 6 m arrangement provides a clean beam dump for the primary proton beam. The M2 magnet is effective to backgrounds from the K_S^0 and Λ decays. Lastly, the M3 magnets are the most important to reduce the background from the Λ decay but less crucial to the background from the K_S^0 decay. The primary proton beam must be dumped upstream of the last magnets so that proton interactions with air between the target and the dump do not introduce backgrounds. The air in the target tube was the principal source of muon antineutrino background in the SSBT neutrino run.

The present design gives a horizontal aperture of ± 4 mrad and a vertical aperture of ± 2 mrad. Computed ν_e (or $\bar{\nu}_e$) fluxes are shown in Figure 8 for incident proton energies of 400, 500 and 1000 GeV. The fluxes are averaged over a radii of 1.35m and 1 m at the 15-Ft. Bubble Chamber and the Wonder Building, respectively. Computed ν_μ fluxes using NUADA for the double

horn system and the bare target (not the SSBT) at the 15-Foot Bubble Chamber with a 1.35m fiducial radius are also shown for comparison.

Relative electron neutrino distributions in the xy plane at the 15-Foot Bubble Chamber and the Wonder Building are shown in Figures 9 and 10 for energy intervals of 40 to 60 and 100 to 120 GeV. The incident proton energy is 400 GeV and each bin is 50 cm. At higher energies the distributions become smaller.

Figures 11 through 14 show ν_e or $\bar{\nu}_e$ fluxes, backgrounds from individual sources and the total ν_μ and $\bar{\nu}_\mu$ backgrounds without the K_L^0 decay contribution at the 15-Foot Bubble Chamber for 400 and 1000 GeV.⁶ Backgrounds for a compromised arrangement which utilizes existing magnets only are also shown for 400 GeV. The target magnet is a Main Ring dipole and the magnet distance is 0.8 in. The backgrounds from the K_S^0 and Λ decay were assumed the same as before.

Muon neutrino flux from the K_L^0 decay⁷ was computed. The spectrum shape is essentially the same as the ν_e spectrum and the flux is 71% of the ν_e flux.

The $\bar{\nu}_\mu$ background from the Λ decay becomes very serious at 1000 GeV as seen in Figure 14. Most of this background comes from Λ decays in the decay pipe and can be reduced by placing magnets further downstream of the present target tube. Computed background from the Λ decay for an arrangement in which a wide gap magnet of 40 cm and 18 kG·m is installed 100 m from the target in the expanded target tube is shown in Figure 14.

REFERENCES

1. Physics interests of electron-neutrino interactions are discussed in various places, for example, in Proposal #566 by C.Baltay and B.P.Roe et al.
2. S.Mori, S.Pruss, and R.Stefanski, TM-725, April 1977.
3. Particle Properties, April 1976, by Particle Data Group.
4. R.Stefanski and H.White, Jr., FN-292, 1976.
5. T.Devlin et al., Nucl.Phys. B123, 1(1977). Inclusive production of K_S^0 has also been measured and reported in this paper. The measured cross sections are in a reasonable agreement with the average K^+ and K^- cross sections computed from Stefanski-White's parametrization.
6. The ν_e flux curve shown for 1000 GeV in Figure 3 of Reference 2 was found incorrect due to an error in the Monte Carlo program.
7. D.W. Carpenter et al., International Conf. on Weak Interactions, October 1965 at ANL, p91.

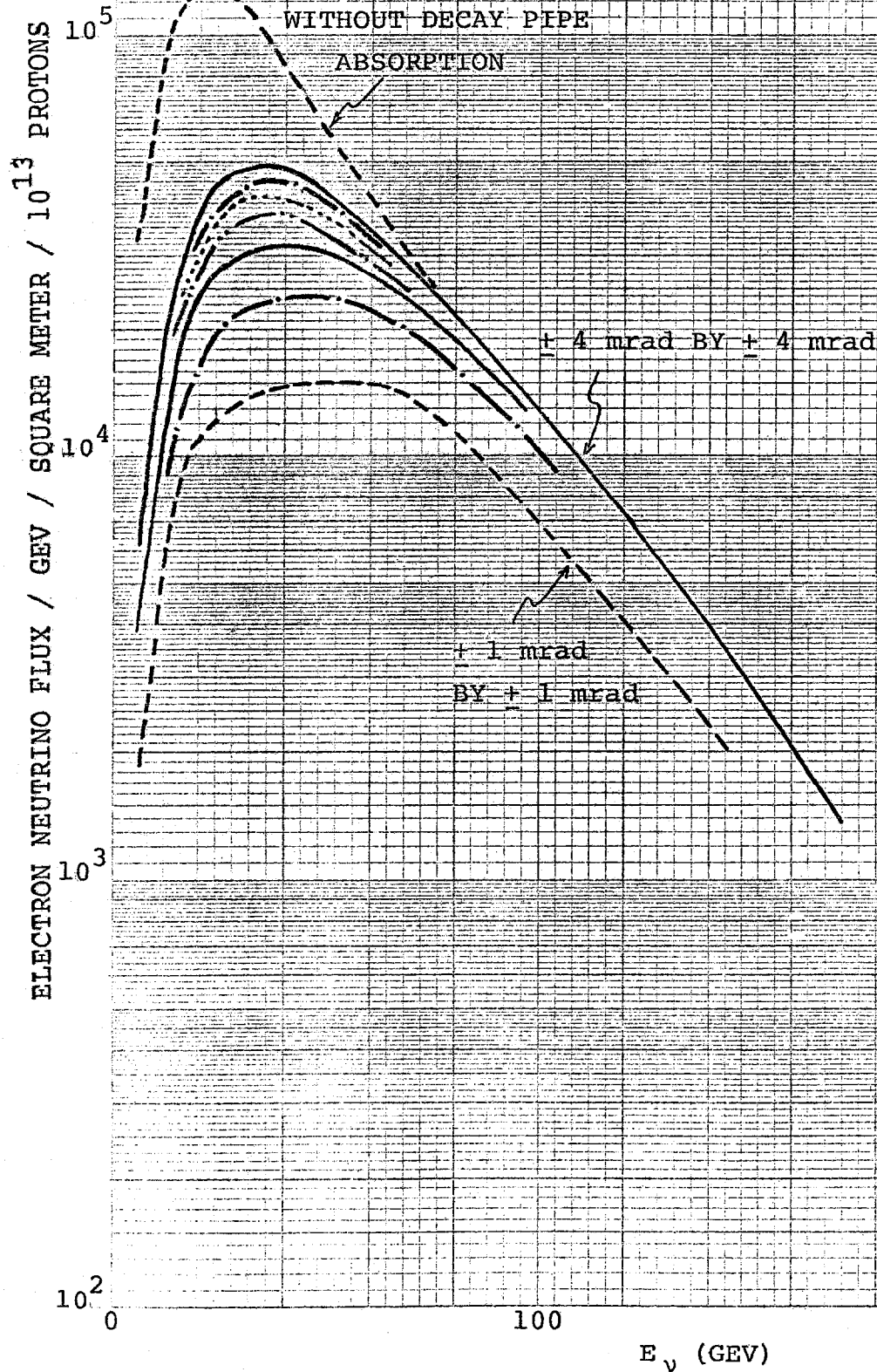
Figure Captions

1. Computed electron neutrino fluxes from the K_L^0 decay as a function of horizontal and vertical apertures for 400 GeV.
2. ν_μ backgrounds from π^+ and K^+ decays for various magnet arrangements of the ν_e beam.
3. Energy distributions of pions, K_S^0 and Λ and pions from K_S^0 and Λ decays. The incident proton energy is 400 GeV.
4. Decay distances for K_S^0 and Λ 's produced at the target for 400 GeV.
5. ν_μ background from the K_S^0 decay, $K_S^0 \rightarrow \pi^+ \pi^- \rightarrow \mu^+ \nu_\mu \pi^-$, for various magnet arrangements.
6. $\bar{\nu}_\mu$ background from the Λ decay, $\Lambda \rightarrow p \pi^- \rightarrow p \mu^- \bar{\nu}_\mu$, for various magnet arrangements.
7. Schematic diagram of the final electron neutrino beam design.
8. Computed electron neutrino fluxes for the final design at the 15-Ft. Bubble Chamber and the Wonder Building. The incident proton energies are 400, 500, and 1000 GeV. Muon neutrino fluxes for the double horn system and the bare target at the 15-Ft. Bubble Chamber are shown for comparison.
9. XY distributions of electron neutrinos from the K_L^0 decay at the 15-Foot Bubble Chamber for 400 GeV. Energy intervals are 40 to 60, and 100 to 120 GeV. Each bin is 50 cm. Cross lines indicate the beam center.
10. XY distributions of electron neutrinos from the K_L^0 decay at the Wonder Building for 400 GeV. Energy intervals are 40 to 60, and 100 to 120 GeV. Each bin is 50 cm. Cross lines indicate the beam center.
11. Computed electron neutrino flux from the K_L^0 decay and ν_μ backgrounds at 15-Foot Bubble Chamber for 400 GeV. The ν_μ backgrounds are shown for the final design of Figure 7 and compromised design with existing magnets only.

12. Computed electron neutrino flux from the K_L^0 decay and $\bar{\nu}_\mu$ backgrounds at the 15-Ft. Bubble Chamber for 400 GeV. The $\bar{\nu}_\mu$ backgrounds are shown for the final design of Figure 7 and a compromised design with existing magnets only.
13. Computed electron neutrino flux from the K_L^0 decay and ν_μ background at the 15-Ft. Bubble Chamber for 1000 GeV.
14. Computed electron neutrino flux from the K_L^0 decay and $\bar{\nu}_\mu$ background at the 15-Ft. Bubble Chamber for 1000 GeV. $\bar{\nu}_\mu$ background from the Λ decay with a wide gap sweeping magnet in the extended target tube, about 100 m from the target is also shown.

ν_e AND $\bar{\nu}_e$ FLUXES FROM THE K_L^0 DECAY
VERSUS APERTURES

INCIDENT PROTON ENERGY = 400 GEV



CURVES BETWEEN ± 4 mrad
AND ± 1 mrad CURVES
ARE FOR ± 3.5 , ± 3 ,
 ± 2.5 , ± 2 , AND
 ± 1.5 mrad FROM THE
TOP.

Figure 1.

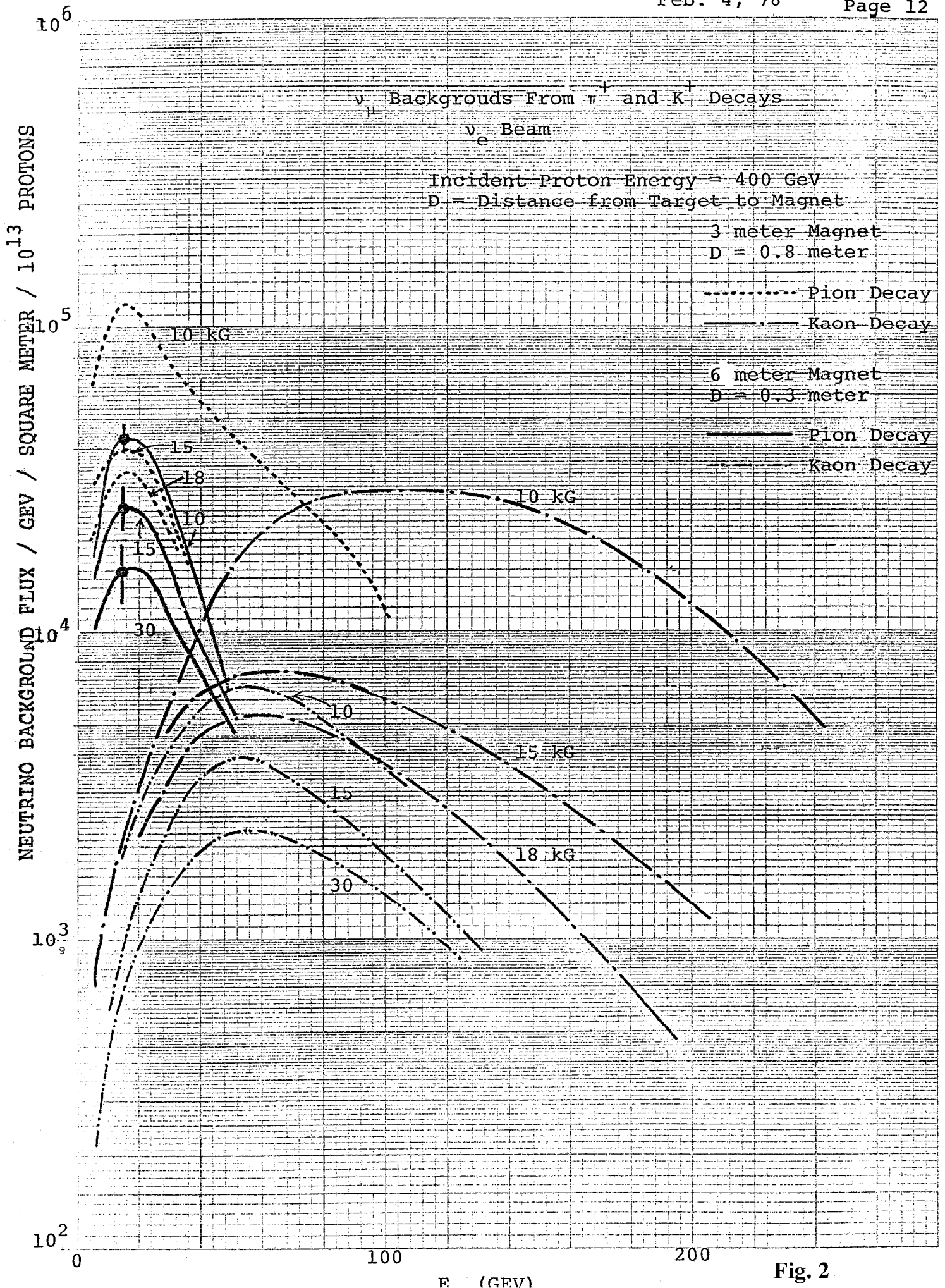


Fig. 2

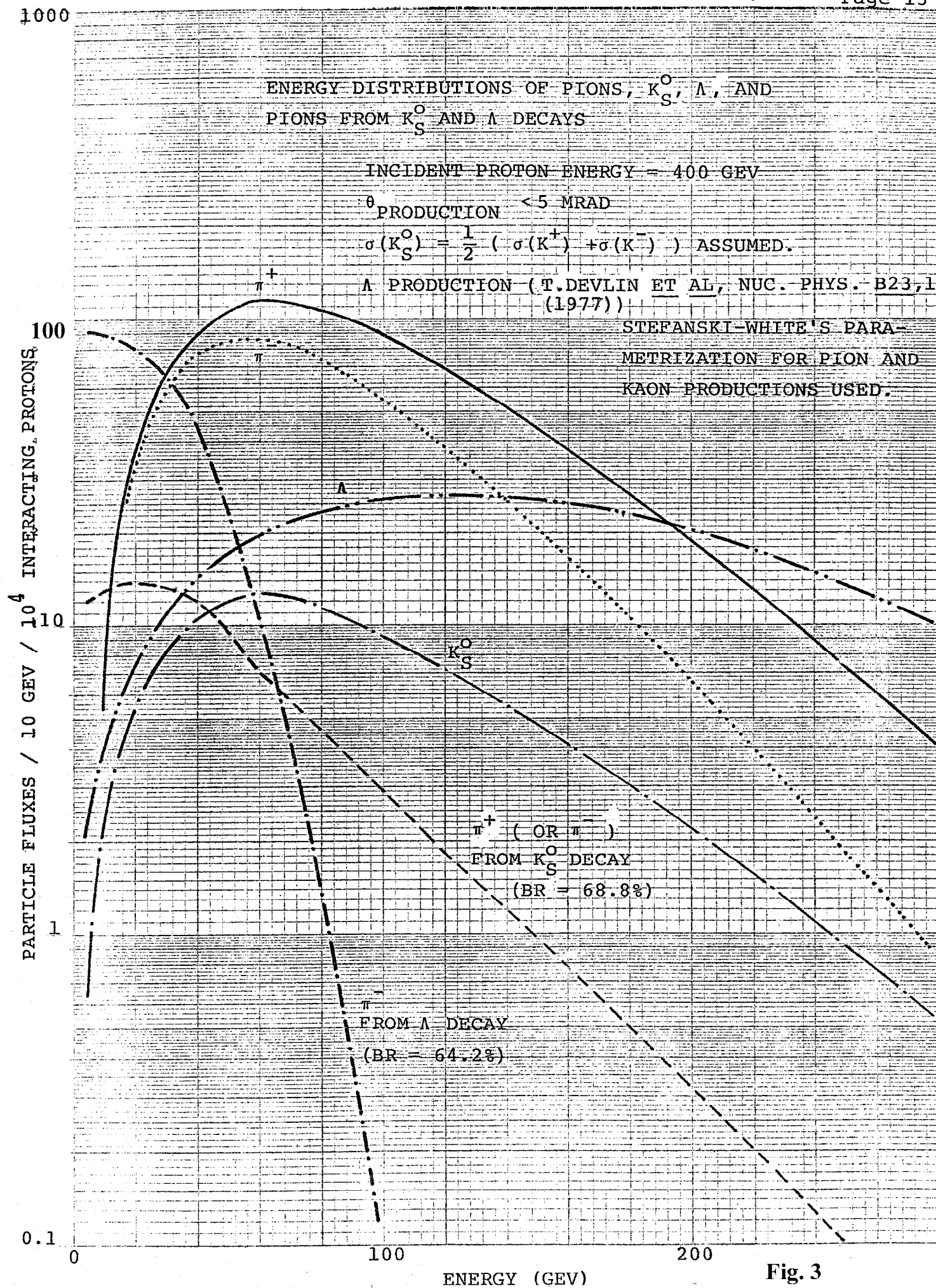
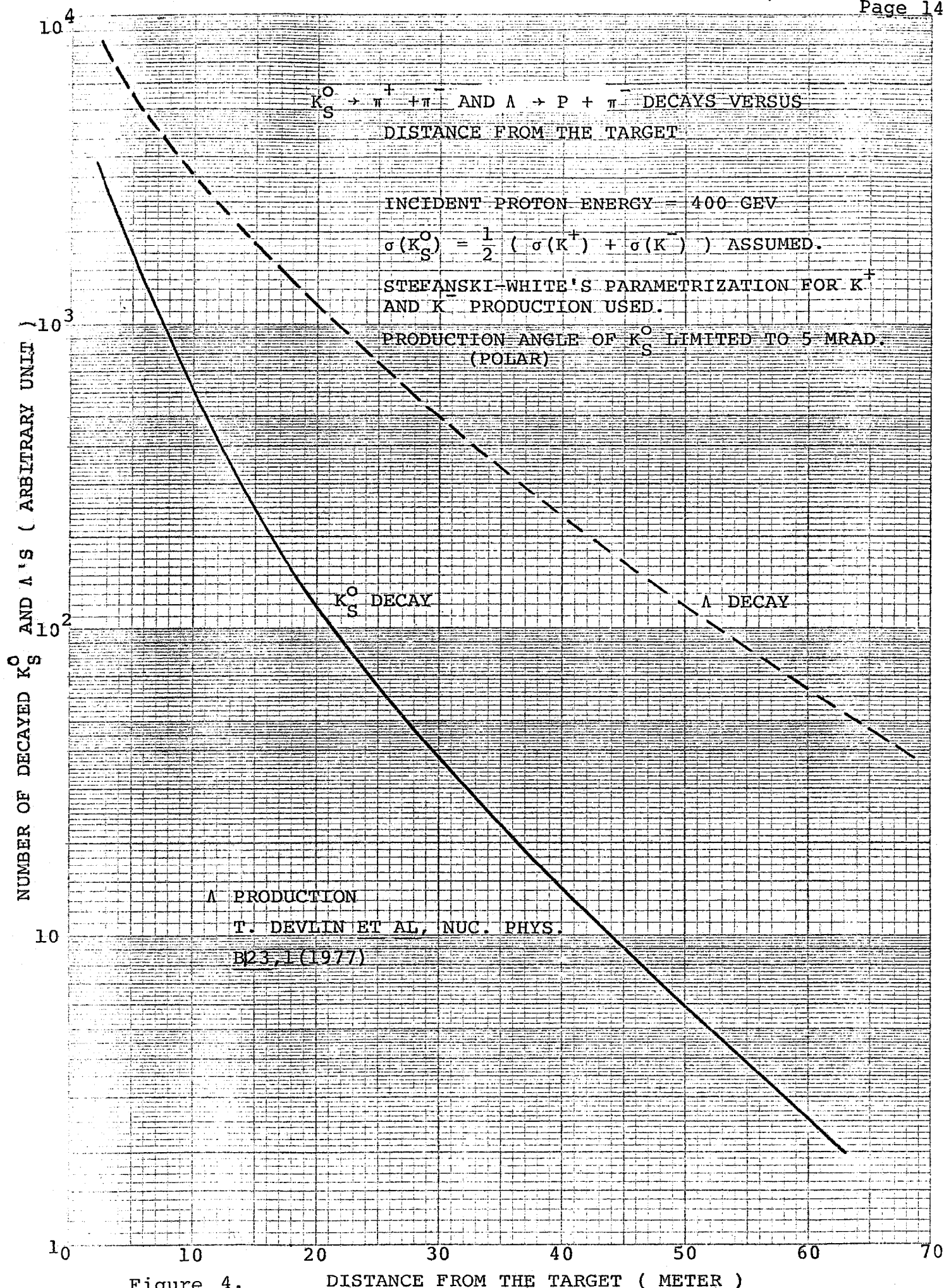


Fig. 3



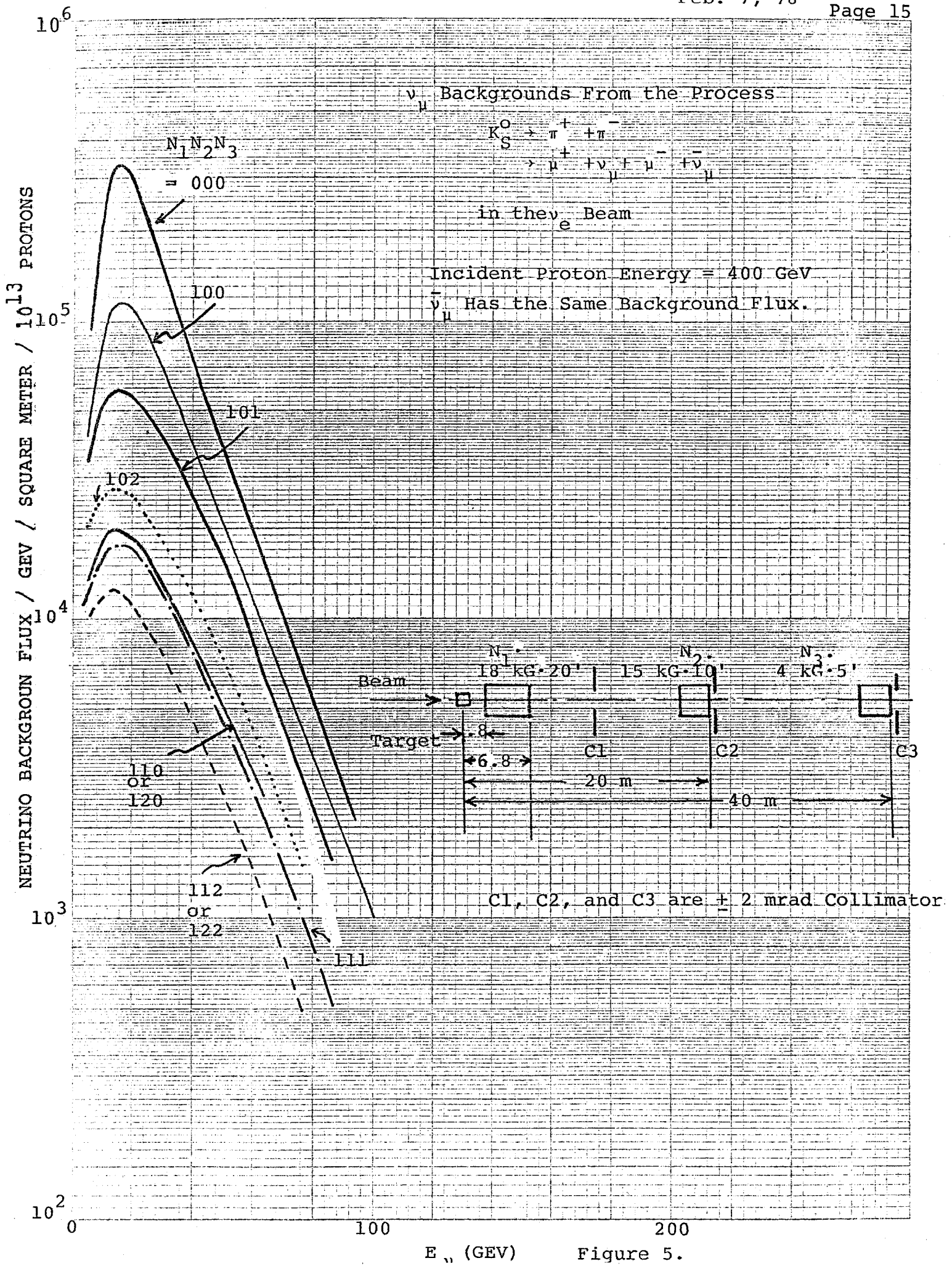


Figure 5.

10^6

$\bar{\nu}_\mu$ BACKGROUND FROM $\Lambda \rightarrow p \pi^-$ DECAY

INCIDENT PROTON ENERGY = 400 GEV

Λ PRODUCTION

T. DEVLIN ET AL, NUCL. PHYS.
B23, 1 (1978)

ISOTROPIC DECAY ASSUMED.

D_{M3} : DISTANCE FROM THE TARGET TO
THE DOWNSTREAM END OF THE
LAST MAGNET.

D_{M1} : DISTANCE FROM THE TARGET TO
THE UPSTREAM END OF THE
FIRST MAGNET.

10^5

$N_1 N_2 N_3$
= 000

111

112

114

112

112

$D_{M1} = 0.8 \text{ M}$

$D_{M3} = 40 \text{ M}$

$D_{M1} = 0.8 \text{ M}$

$D_{M3} = 50 \text{ M}$

$D_{M1} = 0 \text{ M}$

$D_{M3} = 50 \text{ M}$

10^4

100

C3 CLOSED

C1 CLOSED

10^3

10^2

0

50

100

E (GEV)

Figure 6.

C1: MAGNET (M1) PROTECTION COLLIMATOR

C2, C3, C4: ± 2 MRAD XY COLLIMATORS (NO COOLING)

DUMPS: 3 METER LONG ALUMINUM BLOCKS (WATER COOLED)

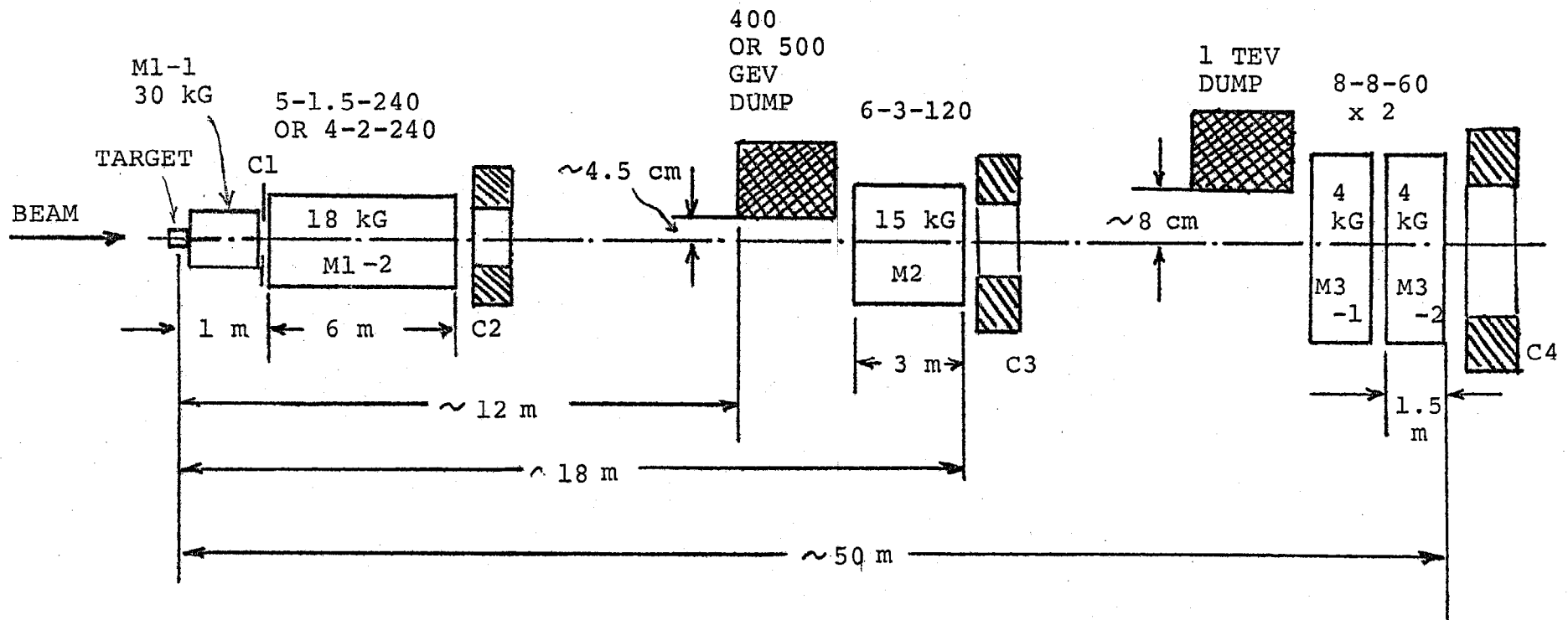


Figure 7.

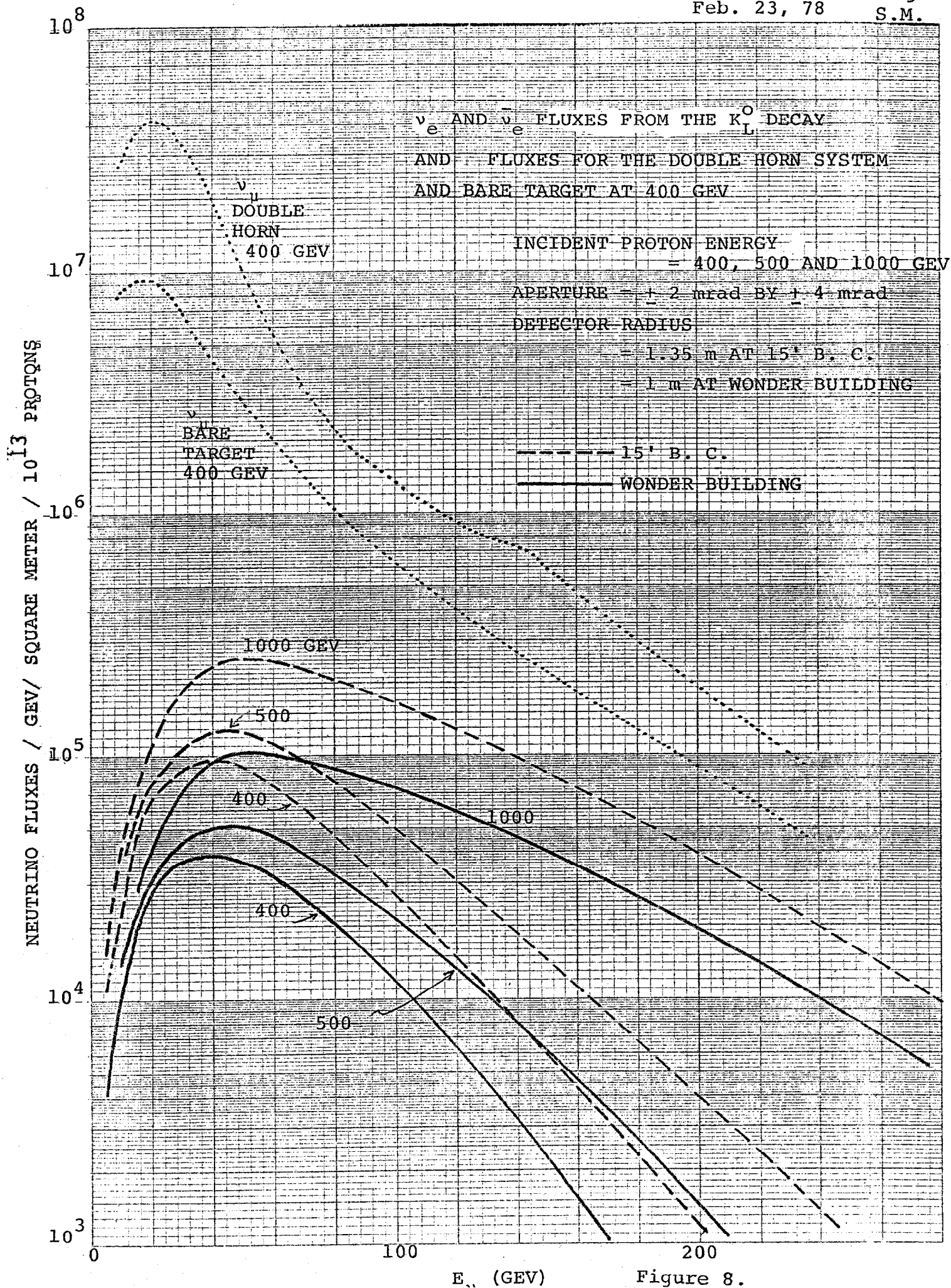


Figure 8.

Page 19

[illegible]

(B) Energy Range = 100 To 120 GeV.

[illegible]

Figure 9. XY Distributions Of Electron Neutrinos From The K_L^0 Decay At The 15' Bubble Chamber For 400 GeV. Each Bin Is 50 cm.

(A) Energy Range = 40 To 60 GeV.

3	6	12	6	9	21	21	20	21	24	17	21	18	12	10	4	4
4	7	19	25	66	207	35	42	35	39	33	17	20	19	7	5	9
13	17	18	17	23	37	62	59	62	47	48	53	45	24	32	14	13
19	15	18	35	47	54	70	70	65	75	78	61	48	35	37	14	12
22	16	31	40	51	59	68	68	65	75	89	51	64	54	38	21	10
14	27	18	44	55	61	79	83	82	76	87	79	86	46	47	17	20
15	24	31	49	80	72	87	83	80	87	77	79	60	61	20	20	11
20	29	43	61	62	76	82	74	87	93	90	65	78	63	48	23	24
18	24	41	45	60	64	61	82	88	102	71	60	81	48	54	36	13
20	26	34	45	48	70	65	83	83	79	107	81	70	61	45	42	16
18	27	34	49	48	60	81	86	84	89	176	84	69	57	53	25	16
18	22	39	37	50	61	64	62	80	73	74	75	62	57	40	35	18
20	17	27	35	40	63	51	67	60	57	51	58	40	39	33	32	19
13	17	12	29	27	33	30	49	68	57	46	46	29	34	30	19	8
13	13	15	14	20	30	39	49	39	57	50	42	33	27	15	14	5
3	7	9	13	20	23	22	28	33	30	25	27	24	24	21	16	7
1	8	16	14	16	17	20	11	21	24	29	23	16	11	8	12	1

(B) Energy Range = 100 To 120 GeV.

0	0	0	0	0	0	0	0	0	1	0	1	0	0	0	0	0
0	0	0	0	0	0	0	0	0	1	1	1	1	0	0	0	0
0	0	0	0	0	0	0	0	0	2	1	1	1	0	0	0	0
0	0	0	0	0	0	0	0	0	4	6	4	4	0	0	0	0
0	0	0	0	0	0	0	0	0	4	6	3	6	1	0	0	0
0	0	0	0	0	0	0	0	0	18	14	13	12	4	1	0	0
0	0	0	0	0	0	0	0	0	25	24	16	12	6	0	0	0
0	0	0	0	0	0	0	0	0	24	30	22	18	3	0	0	0
0	0	0	0	0	0	0	0	0	26	17	16	14	7	0	0	0
0	0	0	0	0	0	0	0	0	26	12	12	15	4	0	0	0
0	0	0	0	0	0	0	0	0	8	17	18	4	0	0	0	0
0	0	0	0	0	0	0	0	0	5	7	3	1	0	0	0	0
0	0	0	0	0	0	0	0	0	5	4	4	1	0	0	0	0
0	0	0	0	0	0	0	0	0	1	2	3	1	1	0	0	0
0	0	0	0	0	0	0	0	0	2	0	1	1	1	0	0	0
0	0	0	0	0	0	0	0	0	1	0	1	1	1	0	0	0
0	0	0	0	0	0	0	0	0	0	0	0	0	0	0	0	0

Figure 10. XY Distributions Of Electron Neutrinos From The K_L^0 Decay
At The Wonder Building For 400 GeV. Each Bin Is 50 cm.

ν_e AND $\bar{\nu}_e$ FLUXES FROM THE K_L^0 DECAY
AND ν_μ BACKGROUNDS AT 400 GEV

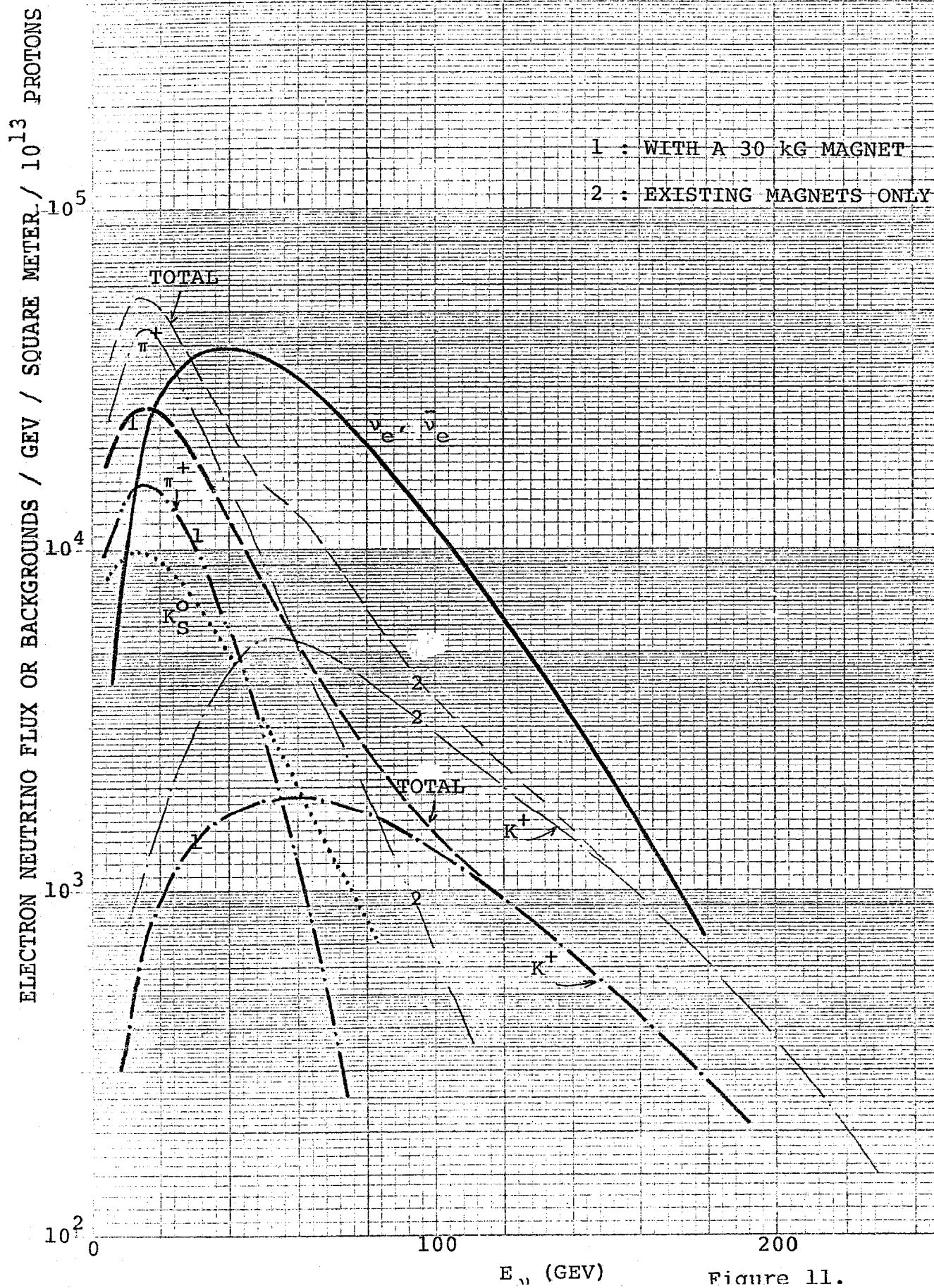
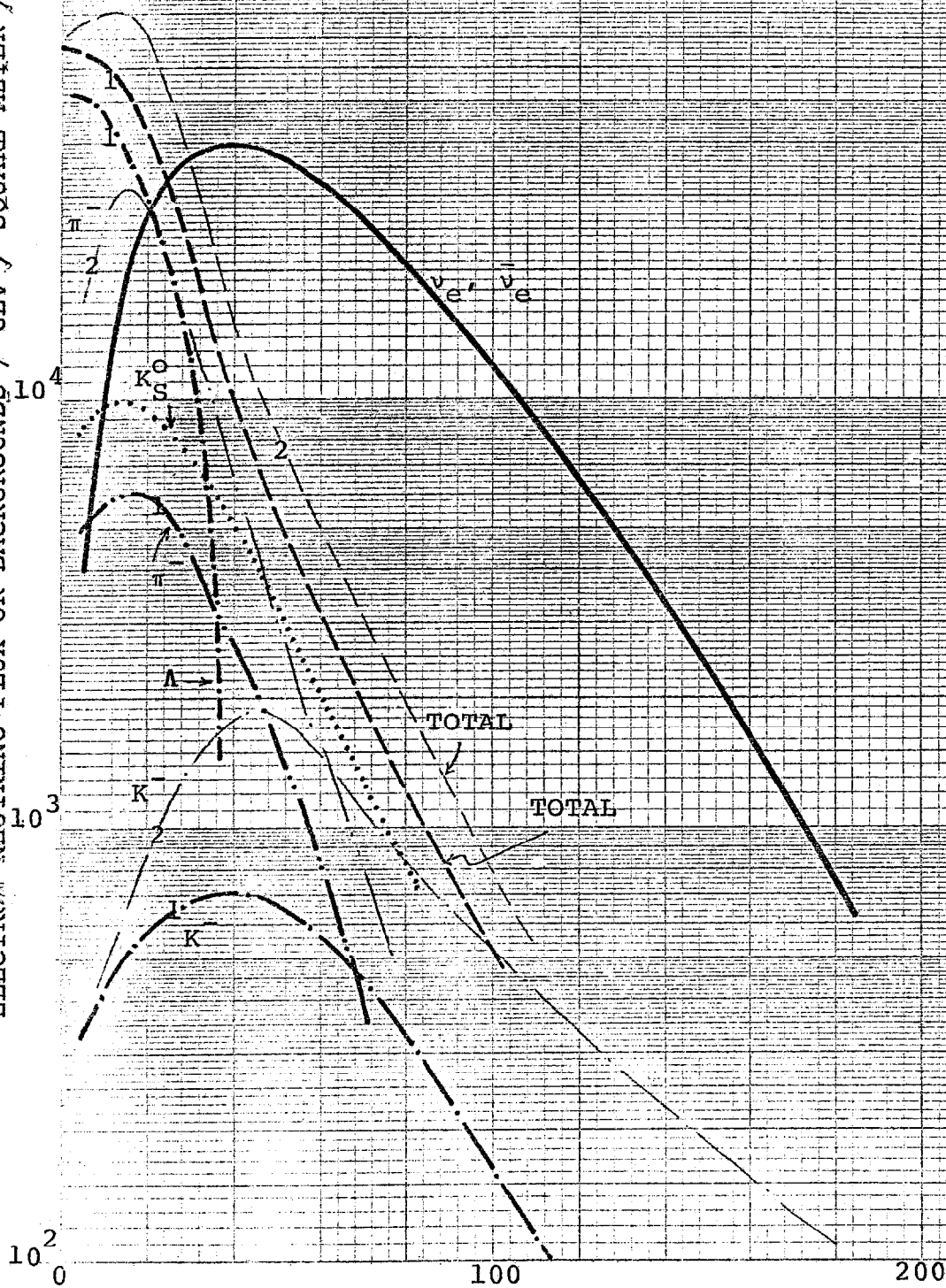


Figure 11.

ELECTRON NEUTRINO FLUX OR BACKGROUNDS / 10^{13} PROTONS / GEV / SQUARE METER

ν_e AND $\bar{\nu}_e$ FLUXES FROM THE K_L^0 DECAY
AND ν_μ BACKGROUNDS AT 400 GEV

1 : WITH A 30 KG MAGNET
2 : EXISTING MAGNETS ONLY



E_ν (GEV)

Figure 12.

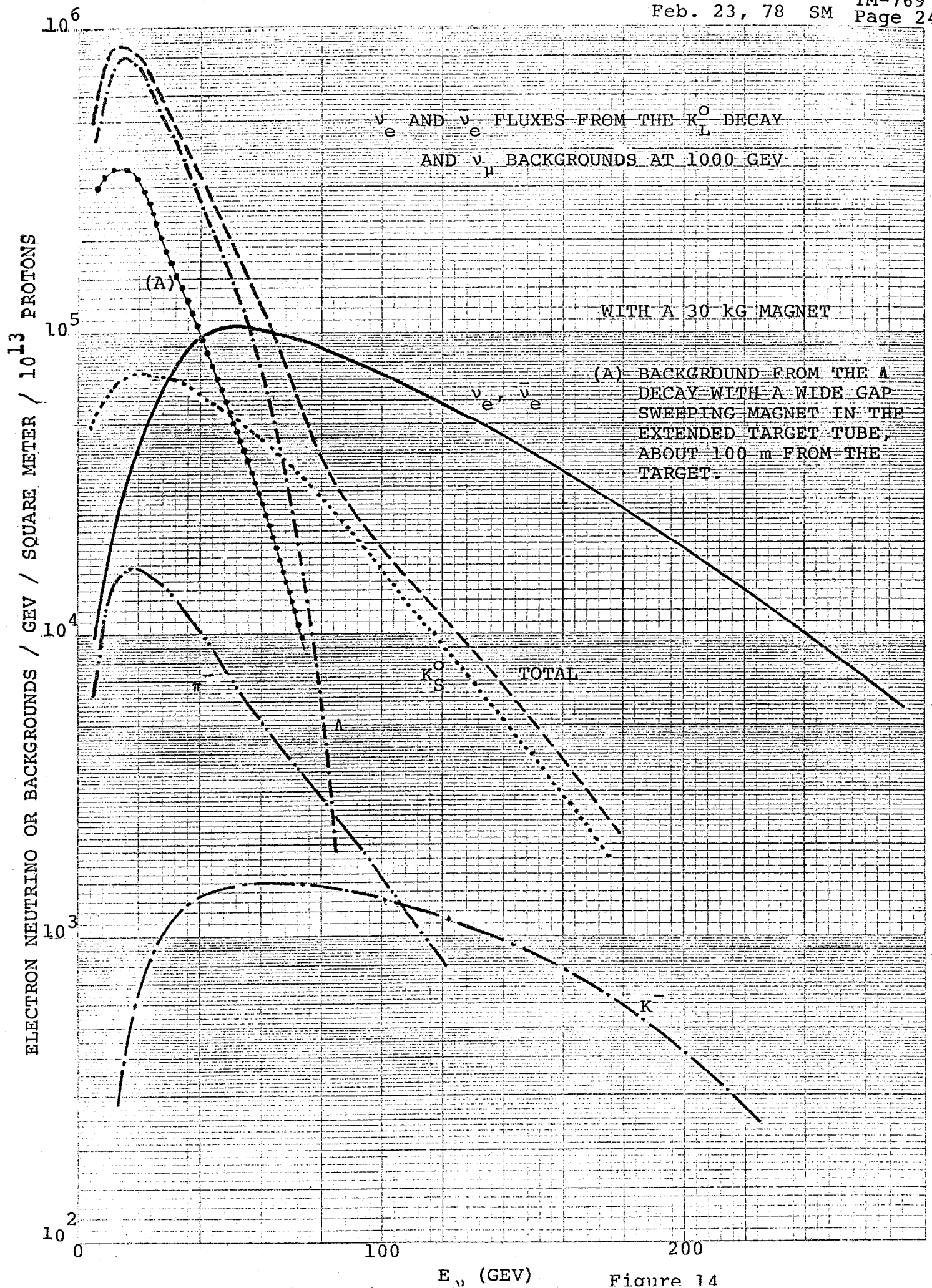


Figure 14

ELECTRON NEUTRINO FLUX OR BACKGROUNDS / GEV / SQUARE METER / 10¹³ PROTONS ν_e AND $\bar{\nu}_e$ FLUXES FROM THE K_L^0 DECAY
AND ν_μ BACKGROUNDS AT 1000 GEV

WITH A 30 KG MAGNET

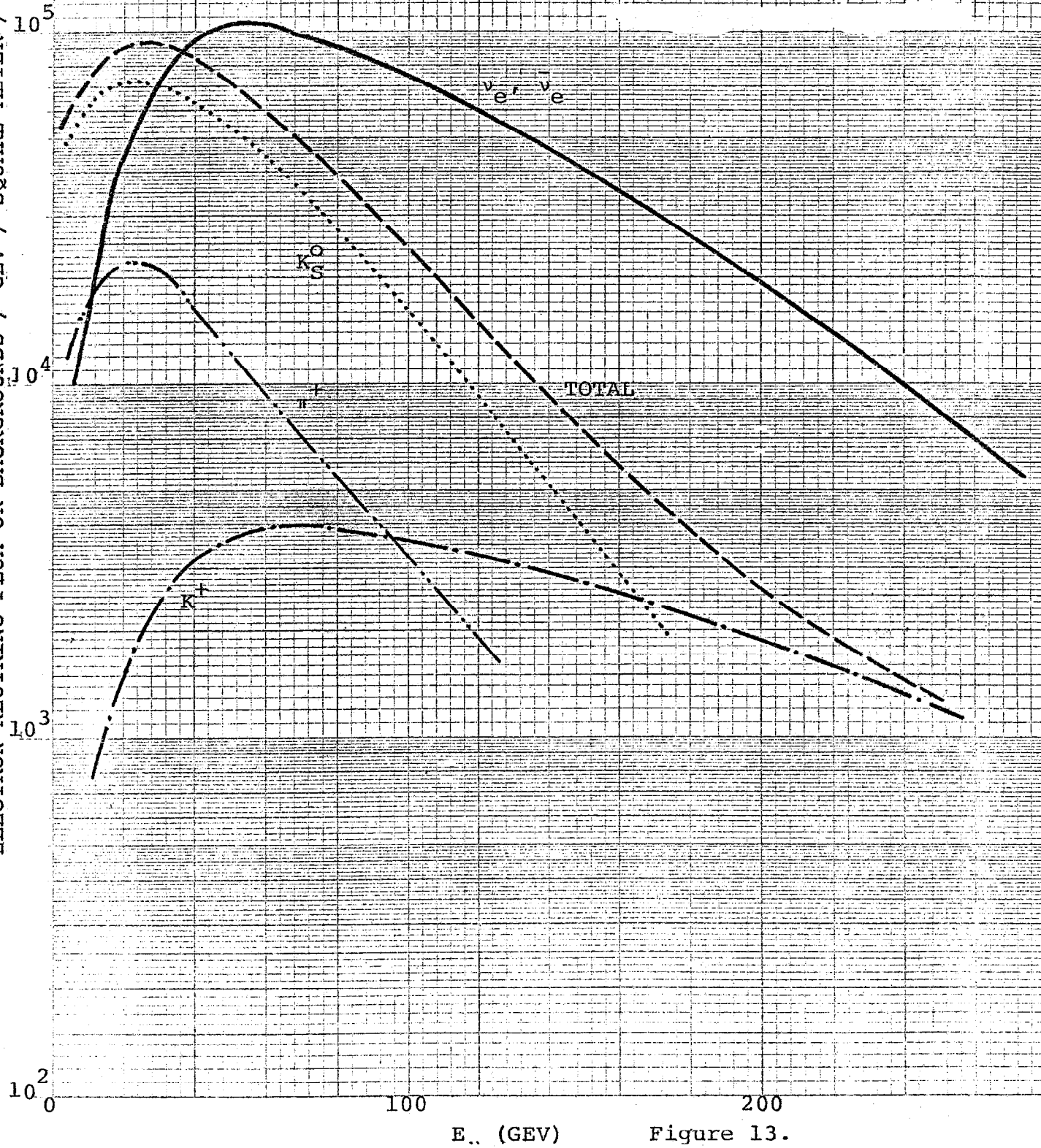


Figure 13.